Catalysis Science & Technology

Cite this: *Catal. Sci. Technol.*, 2012, **2**, 767–772

www.rsc.org/catalysis

PAPER

The average Pd oxidation state in Pd/SiO_2 quantified by L_3-edge XANES analysis and its effects on catalytic activity for CO oxidation†

Ken-ichi Shimizu,*[a] Yuichi Kamiya,[b] Kaoru Osaki,[c] Hisao Yoshida[d] and Atsushi Satsuma[c]

Received 14th October 2011, Accepted 16th December 2011
DOI: 10.1039/c2cy00422d

The palladium oxidation state of an SiO_2-supported palladium catalyst was quantitatively determined by Pd L_3-edge XANES (X-ray absorption near-edge structure) analysis. By changing the time of CO-reduction pre-treatment at 673 K, a series of 5 wt% Pd-loaded SiO_2 catalysts ($PdO_{x/2}/SiO_2$) containing different amounts of the Pd metal and PdO phases were prepared, and the average oxidation number (x) was estimated from the number of CO_2 molecules formed during the CO-reduction treatment. L_3-edge XANES spectra of these samples and a reference sample (Pd powder) were recorded, and the white line area of the spectra was evaluated. A good linear relationship was confirmed between the white line area intensity and the average oxidation number (x), indicating that the oxidation state of Pd in structurally unknown Pd samples could be quantitatively determined by a simple XANES analysis. To demonstrate the utility of this method in a catalytic study, the effect of the oxidation number (x) on the CO oxidation activity of $PdO_{x/2}/SiO_2$ was also examined, and metallic Pd^0 sites in $PdO_{x/2}/SiO_2$ were shown to be active species.

Introduction

Pt, Pd, and Rh have been indispensable elements in industrial heterogeneous catalysts[1–18] for electrocatalysis, hydrogenation, oxidation, and automotive catalysis. Toward a knowledge-based development of metal catalysts, fundamental studies of the correlation between structure (size, shape, and oxidation state) and reactivity have been an important topic in catalysis. For the oxidation of CO and hydrocarbons, the oxidation state of metal species strongly affects the activity of supported Pt,[3–10] Pd,[11–16] and Rh[17,18] catalysts. The effect of Pt oxidation state on the activity has been most extensively studied. Generally, Pt in the metallic state shows higher catalytic performance than in the oxidized state. However, a few reports showed that partially oxidized Pt exhibited higher activity than the metallic one.[7] For supported Pd catalysts, Yazawa *et al.*[11] studied the relation between the Pd oxidation state and their catalytic activity for propane combustion and concluded that partially oxidized Pd was effective. Newton and co-workers[14] recently demonstrated that the Pd(I) and Pd(0) sites are active species of Al_2O_3-supported Pd with Pd particle size 2.5 nm and 3.5 nm, respectively, for CO elimination under $CO/(NO + O_2)$ cycling conditions. These examples demonstrate that the oxidation state of the active metal species depends on the structural factors (type of metals and support materials and particle size) and the reaction conditions, and hence, continuous efforts should be devoted to elucidate the effect of the metal oxidation state on the catalytic activity. For this purpose, the oxidation states of Pt, Pd, and Rh should be conveniently and accurately estimated. Although XPS (X-ray photoelectron spectroscopy) has been the most commonly used method for this purpose, the XPS spectra of metal catalysts containing the metal species of various oxidation states generally give a poorly resolved broad feature.[11,15,18]

X-Ray absorption spectroscopy (XAS) is a powerful method to characterize the electronic state of metal catalysts.[19] The white line feature at L_3-edge X-ray absorption near-edge structures (XANES) of transition metal compounds is typically assigned to electron transition from $2p_{3/2}$ to $5d_{3/2}$ and $5d_{5/2}$, and hence the area of the white line can be an index for the oxidation state of the transition metals. Most of the L_3-edge XANES studies of heterogeneous catalysts have been focused on 5d transition metals.[1–10,20–22] In contrast, few attempts have been focused on L_3-edge XAS studies of 4d (Pd,[23–27] Ag,[28] Rh[29]) and 3d (Cu,[30] Co[31]) transition metals-based catalysts. Previously, Chen *et al.*[32] reported a XANES study of the electronic structure of 4d transition metals (Mo, Tc, Ru, Pd, Ag) and showed that the white line area intensity of them increased linearly with increasing

[a] *Catalysis Research Center, Hokkaido University, N-21, W-10, Sapporo 001-0021, Japan. E-mail: kshimizu@cat.hokudai.ac.jp; Fax: +81-11-706-9163*
[b] *Research Faculty of Environmental Earth Science, Hokkaido University, Kita 10 Nishi 5, Sapporo 060-0810, Japan*
[c] *Department of Molecular Design and Engineering, Graduate School of Engineering, Nagoya University, Nagoya 464-8603, Japan*
[d] *Department of Applied Chemistry, Graduate School of Engineering, Nagoya University, Furo-cho, Chikusa-ku, Nagoya 464-8603, Japan*
† Electronic supplementary information (ESI) available. See DOI: 10.1039/c2cy00422d

atomic number. The result illustrates the proportionality of the 4d-hole count to the white line area. Yoshida *et al.*[4] demonstrated that the white line area at Pt L_3-edge XANES increased linearly with increase in the O/Pt ratio in various Pt catalysts, indicating a quantitative correlation between the Pt oxidation state and the white line area intensity. Although Pd is an important element in oxidation catalysis, to the best of our knowledge, there are quite a few Pd L_3-edge XANES studies of Pd catalysts for catalytic oxidation. Recently, we have reported a simple method of Rh L_3-edge XANES analysis to quantify the oxidation states of Rh species in a series of supported Rh catalysts containing different amounts of Rh metal and Rh_2O_3 phases.[29] A linear relationship between the average oxidation numbers determined by a chemical method (the number of CO_2 molecules formed during pre-reduction by CO) and the white line intensities at the L_3-edge Rh verifies that this method is effective for quantification of the average Rh oxidation number in structurally unknown Rh samples. In the present study, the same research strategy was applied to establish a Pd L_3 edge XANES analysis for the quantification of the average Pd oxidation state (x) of Pd species in $PdO_{x/2}/SiO_2$ samples. A linear relationship between these values will verify the quantitative correlation between the Pd oxidation state and the white line area intensity. These samples are characterized by conventional methods (Pd K-edge XANES/EXAFS and XRD), and the advantages of Pd L_3-edge XANES are discussed. To demonstrate the utility of this method in a catalytic study, we also study the effect of the Pd oxidation state on the catalytic activity of the $PdO_{x/2}/SiO_2$ samples for CO oxidation.

2. Experimental

2.1. Catalyst preparation

Pd(5 wt%)-loaded SiO_2 catalysts were prepared by impregnating SiO_2 (Q-10, Fuji Silysia Chemical Ltd., 300 m^2 g^{-1}) with aqueous HNO_3 solution of $Pd(NO_3)_2$, followed by evaporation to dryness at 353 K, drying at 393 K for 12 h, calcination in air at 973 K for 1 h. As shown below, Pd species existed as PdO in the as-calcined catalyst, referred to as PdO/SiO_2. This oxidized sample was finally reduced at 673 K in a flow of 0.4% CO/He (flow rate = 100 cm^3 min^{-1}), and the gas formed during the CO-reduction treatment was continuously analyzed by nondispersive infrared CO/CO_2 analyzers (Horiba VIA510). By changing the time (0, 1, 2, 7, 10 min) of this CO-reduction treatment, a series of $PdO_{x/2}/SiO_2$ catalysts with different average oxidation numbers of Pd (x) were prepared as summarized in Table 1.

2.2. Characterization

X-Ray diffraction (XRD) patterns of the powdered catalysts were recorded with a Rigaku MiniFlex II/AP diffractometer with Cu Kα radiation. By using Si powder as an internal standard, the XRD intensity of different $PdO_{x/2}/SiO_2$ samples was normalized. The number of surface metal atoms in the fully reduced sample (Pd/SiO_2) was estimated with the CO uptake of the samples at 195 K,[33] after reducing the catalyst surface in H_2 at 473 K, by the pulse-adsorption of CO in a flow of He. The average particle size was calculated from the CO uptake assuming that CO was adsorbed on the surface of spherical Pd particles at a CO/(surface Pd atom) ratio of 1/1.

Table 1 Preparation conditions and structural information of the catalysts

Catalysts	t_{CO}/min[a]	x[b]	D/nm[c]	L_3 WL area (a.u.)[d]
PdO/SiO_2	0	2.0	14.8	12.4
$PdO_{0.8}/SiO_2$	1	1.6	—	10.8
$PdO_{0.6}/SiO_2$	2	1.3	—	10.1
$PdO_{0.1}/SiO_2$	7	0.24	—	7.1
Pd/SiO_2	10	0	21.1	6.9
Pd powder	—	0	—	6.9

[a] Time of CO-reduction treatment at 673 K. [b] Average oxidation number of supported Pd species estimated from CO_2 formation during the CO-reduction at 400 °C. [c] Average particle size of Pd or PdO from XRD analysis. [d] White line area intensity at L_3-edge after subtraction of the continuum absorption.

Pd K-edge XAS measurement was carried out in a transmission mode with a Si(111) monochromator at BL14B2 of SPring-8 (Hyogo, Japan) operated at 8 GeV. The analyses of the extended X-ray absorption fine structure (EXAFS) and XANES were performed using the REX version 2.5 program (RIGAKU). The Fourier transformation of the k^3-weighted EXAFS from k space to R space was carried out over the k range 2.5–15 $Å^{-1}$. A part of the Fourier-transformed EXAFS in the R range of 1.0–3.6 Å were inversely Fourier-transformed, followed by the analysis with a usual curve fitting method in the k range of 2.5–14.0 $Å^{-1}$. The parameters for the Pd–Pd and Pd–O shells were provided by the FEFF6. The number of free parameters[34] for curve fitting can be estimated as $P_{free} = 2\Delta k\Delta R/\pi \approx 20$, indicating that we can model the EXAFS data with five shells.

Pd L_3-edge XANES spectra were obtained at the BL-9A station of the KEK-PF (Tsukuba, Japan) with a ring energy of 2.5 GeV and a stored current of 250–350 mA. The spectra were recorded in a transmission mode at room temperature with a Si(111) double-crystal monochromator. The background subtraction and normalization were performed by REX version 2.5. The white line area of normalized Pd L_3-edge XANES spectrum was evaluated by subtracting the normalized XANES spectrum by an arctangent function, eqn (1):[4,30]

$$a(E) = h[0.5 + \pi^{-1}\tan^{-1}\{(E - E_0)/\omega\}], \quad (1)$$

where E: X-ray energy (eV), $a(E)$: arctangent function, h: height, ω: width, E_0: inflection point (eV). In the present simulation, h_1 was 1 and ω_1, which should be related to the natural width of the 2p electron and the experimental conditions, was fixed as 0.33.[4,30] Note that changes in the ω_1 value in a range of 0.2–0.5 resulted in negligible changes in the white line area intensity (below ±0.6%). The value of E_0 was assumed to be the same as the peak position of the white line.

2.3. CO oxidation

Catalytic CO oxidation was performed in a fixed-bed flow reactor (inner diameter = 4 mm) at 413 K. A gas mixture of CO/O_2/He (0.46%/10%/balance) was fed to the catalyst (5 mg) at a flow rate of 100 cm^3 min^{-1}. The effluent gas was analyzed by nondispersive infrared CO/CO_2 analyzers (Horiba VIA510). Reaction rates per gram of the $PdO_{x/2}/SiO_2$ catalysts for the

CO oxidation were estimated under the conditions where CO conversion was below 15%.

3. Results and discussion

3.1. Conventional characterizations

Structural information derived from various characterization experiments is summarized in Table 1. The crystal phase was confirmed by XRD (Fig. 1). In the XRD pattern of the as-calcined sample, PdO/SiO_2, lines due to the Pd metal were absent, and broad lines assignable to PdO were observed. By changing the time of CO-reduction pre-treatment at 673 K, we prepared a series of $PdO_{x/2}/SiO_2$ samples with various oxidation states. The average oxidation number (x) was estimated from the amount of CO_2 molecules formed during the CO reduction treatment, according to the following stoichiometry: $x/2CO + PdO_{x/2} = x/2\ CO_2 + Pd$. As expected, the oxidation number (x) decreased with the time of CO-reduction, accompanying a decrease in the diffraction intensity of the PdO phase and an increase in that of the Pd metal. The number of CO_2 molecules formed during CO-reduction at 673 K for 10 min corresponds to a completely reduced $PdO_{x/2}/SiO_2$ ($x = 0$) sample, thus the sample is referred to as Pd/SiO_2. The result is consistent with the XRD result of this sample; there is a diffraction line due to the Pd metal but no diffraction lines due to PdO. Normalized XRD intensity due to the Pd metal or PdO is plotted as a function of the oxidation number (x) in Fig. 1b. It is qualitatively shown that the PdO/Pd ratio increases with x, but the result in Fig. 1b does not give a quantitative conclusion. The average crystallite size of the Pd metal in the Pd/SiO_2 sample and PdO in the PdO/SiO_2 sample was calculated from the half-width of the diffraction lines at 40.12° and 33.88°, respectively, in the XRD patterns using the Scherrer equation. The average size of the Pd metal in Pd/SiO_2 (21.1 nm) was larger than that of PdO in PdO/SiO_2 (14.8 nm). In summary, five kinds of the $PdO_{x/2}/SiO_2$ samples with different average oxidation numbers but with the same Pd loading (5 wt%) were prepared as listed in Table 1.

Fig. 2 shows Fourier transforms of k^3-weighted Pd K-edge EXAFS, and Table 2 shows curve-fitting results. Peaks appearing at 1–2 Å are due to the adjacent oxygen atoms, and peaks at 2–3.5 Å are due to Pd atoms in Pd or PdO. The values of the coordination numbers for Pd–O and Pd–Pd species as well as the distances (EXAFS analysis) are listed in Table 2. The EXAFS of the PdO/SiO_2 sample consists of a

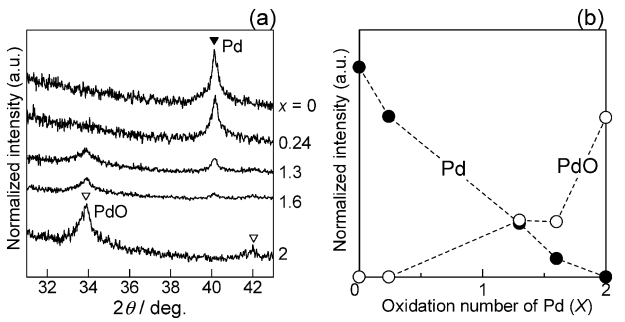

Fig. 1 (a) X-ray diffraction patterns of the $PdO_{x/2}/SiO_2$ samples with different average oxidation numbers (x). (b) Normalized XRD intensity due to Pd metal or PdO *vs.* x.

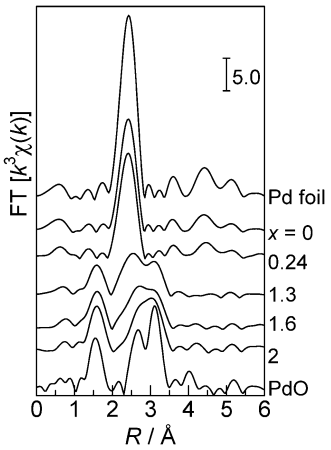

Fig. 2 Fourier transforms of Pd K-edge EXAFS for the reference compounds and the $PdO_{x/2}/SiO_2$ samples with different average oxidation numbers (x).

Pd–O contribution with a coordination number (CN) of 3.0 at a bond distance (R) of 2.02 Å and two Pd–Pd contributions: CN = 3.0 at R = 3.04 Å and CN = 4.4 at R = 3.42 Å. These Pd–O and Pd–Pd distances are consistent with the crystallographic data for PdO. The EXAFS of the Pd/SiO_2 sample consisted of a Pd–Pd contribution of CN = 7.7 at R = 2.74 Å, which is nearly close to the crystallographic data of the Pd–Pd distance in the Pd metal (2.74 Å). These results are consistent with the results from the XRD analysis. Considering the crystallographic data of Pd and PdO (Table 2) and the XRD results, the EXAFS of the $PdO_{0.8}/SiO_2$, $PdO_{0.6}/SiO_2$ and $PdO_{0.1}/SiO_2$ samples could be fitted with four shells: a Pd–O shell at 2.02 Å and three Pd–Pd shells at the second (2.74 Å), the third (3.04 Å) and the fourth (3.42 Å) coordination spheres. The curve-fitting with the four shells was successful for the $PdO_{0.8}/SiO_2$ and $PdO_{0.6}/SiO_2$ samples. However, for $PdO_{0.1}/SiO_2$, the curve-fitting with two shells gave a good fitting value (R_f in Table 2), and increase of the number of

Table 2 Curve-fitting analysis of Pd L_3-edge EXAFS

Sample	Shell	CN[a]	R/Å[b]	σ/Å[c]	R_f (%)[d]
PdO/SiO_2	O	3.0	2.02	0.047	1.2
	Pd	3.0	3.04	0.064	
	Pd	4.4	3.42	0.059	
$PdO_{0.8}/SiO_2$	O	2.7	2.03	0.046	1.0
	Pd	1.4	2.74	0.089	
	Pd	3.1	3.04	0.071	
	Pd	4.1	3.42	0.067	
$PdO_{0.6}/SiO_2$	O	2.1	2.03	0.038	1.1
	Pd	2.1	2.74	0.078	
	Pd	3.1	3.04	0.077	
	Pd	3.1	3.42	0.060	
$PdO_{0.1}/SiO_2$	O	0.5	2.02	0.059	0.8
	Pd	7.2	2.73	0.079	
Pd/SiO_2	Pd	7.7	2.74	0.080	0.8
PdO	O	(4)[e]	(2.02)[e]	—	—
	Pd	(4)[e]	(3.04)[e]	—	—
	Pd	(8)[e]	(3.42)[e]	—	—
Pd metal	Pd	(12)[e]	(2.74)[e]	—	—

[a] Coordination number. [b] Bond distance. [c] Debye–Waller factor. [d] Residual factor. [e] Crystallographic values (ICSD #29281 for PdO, ICSD #64916 for the Pd metal).

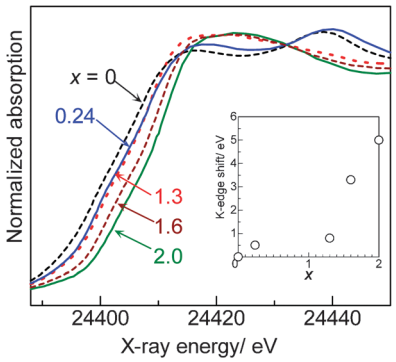

Fig. 3 Pd K-edge XANES spectra of $PdO_{x/2}/SiO_2$ catalysts with different average oxidation numbers (x). A plot of K-edge energy *vs.* x is given as an inset.

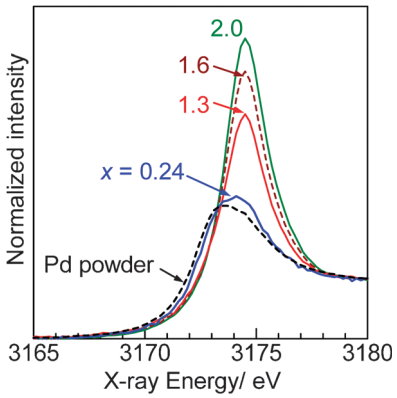

Fig. 4 Pd L_3-edge XANES spectra of the representative $PdO_{x/2}/SiO_2$ samples with different average oxidation numbers (x) and Pd powder.

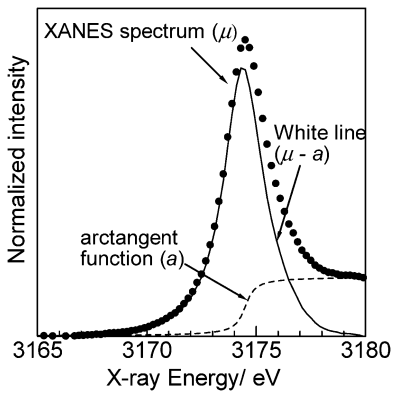

Fig. 5 Example for a method for Pd L_3-edge XANES analysis. The spectrum was for the PdO/SiO_2 sample. An arctangent function (dashed line) for the continuum absorption is subtracted from the raw spectrum (dots) to give a function corresponding to the white line peak (solid line).

Pd–Pd shells did not improve the fitting value. There are general tendencies that a decrease in the oxidation number (x) in the $PdO_{x/2}/SiO_2$ samples results in decreases in the CN of the Pd–O shell and the Pd–Pd shells at 3.04 and 3.42 Å and an increase in the CN of the Pd–Pd shell at 2.73–2.74 Å. This supports that the PdO/Pd ratio decreases with increase in x. For the $PdO_{x/2}/SiO_2$ (x = 2, 1.6, 1.3) samples, the ratio of CN values for the Pd–Pd shells at 3.04 Å and 3.42 Å is not consistent with the crystallographic value. Considering the above problems in the curve-fitting analyses, we can conclude that EXAFS analysis is useful to estimate a trend in the PdO/Pd ratio qualitatively but is not useful for a quantification of the PdO/Pd ratio as an index of the average oxidation state of Pd species.

It is established that the K-edge threshold energy shifts to higher energy as the oxidation number of the X-ray absorbing atom is increased. Pd K-edge XANES spectra of the $PdO_{x/2}/SiO_2$ samples are shown in Fig. 3. In this study, the threshold was defined as the point at which intensity was 0.4 in the normalized XANES spectra. The threshold energy, which would be an indicator for the Pd oxidation state, is plotted in an inset of Fig. 3 as a function of x. Qualitatively, there is a tendency that an increase in the oxidation number (x) in the $PdO_{x/2}/SiO_2$ samples results in an increase in the K-edge energy. However, a poor correlation between x and the threshold energy indicates that the K-edge XANES shift is not useful in the quantitative determination of the average oxidation state of the $PdO_{x/2}/SiO_2$ samples.

3.2. Quantification of the Pd oxidation state by L_3-edge XANES analysis

Pd L_3-edge absorption spectra of the $PdO_{x/2}/SiO_2$ samples and Pd powder are shown in Fig. 4. As previously reported by Chen *et al.*,[32] the XANES spectrum of Pd powder, a reference compound of metallic Pd, showed a small while line due to lack of the 4d-hole. In contrast, the XANES spectrum of the PdO/SiO_2 sample exhibited a large white line peak at 3174.5 eV with a symmetric shape. This peak should be predominantly assignable to the electron transition from $2p_{3/2}$ to $5d_{3/2}$ and $5d_{5/2}$, and hence, it is expected that the area intensity of the white line can be an index for the oxidation state of Pd species. As the average oxidation number (x) of the $PdO_{x/2}/SiO_2$ samples increased, the area intensity of the white line increased, indicating an increase of vacancy in the d-states. Adopting the method in our previous study[29] for the Rh L_3-edge XANES analysis, the area intensity of the white line was determined as illustrated in Fig. 5. An arctangent function shown as a dashed line, which corresponds the continuum absorption, is subtracted from the raw spectrum (dots) to give a function corresponding to an absorption predominantly related to the electron transition from $2p_{3/2}$ to $5d_{3/2}$ and $5d_{5/2}$ (solid line). The white line area intensities thus estimated were listed in Table 1, and also plotted as a function of the average oxidation number of the $PdO_{x/2}/SiO_2$ samples and Pd powder as shown in Fig. 6. It is found that the white line area intensity increased linearly with the oxidation number. This clearly indicates that the white line area intensity at the Pd L_3-edge XANES is a quantitative index of the Pd oxidation state. Therefore, it is concluded that the present method of Pd L_3-edge XANES analysis can be used for the quantitative estimation of the average oxidation number of unknown Pd species. Taking into account the fact that conventional XPS spectra of Pd samples containing Pd species of different oxidation states give a poorly resolved broad feature,[11] this method would be widely acceptable as a novel characterization method for a quantification of the Pd oxidation states. Since this

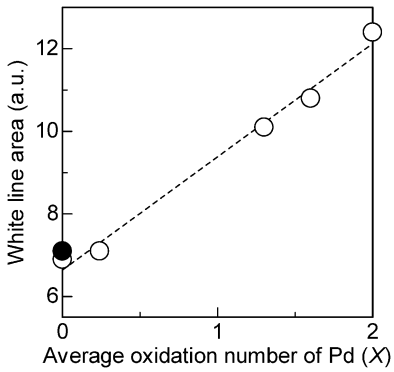

Fig. 6 Relation between the average oxidation number (x) and the white line area intensity of the Pd L_3-edge XANES of (○) the $PdO_{x/2}/SiO_2$ samples and (●) Pd powder.

method is based on the 4d-hole, this will become generally applicable to determination of the oxidation state of various Pd compounds.

3.3. Structure–activity relationship

To demonstrate the utility of Pd L_3-edge XANES analysis in a catalytic study, the effect of the Pd oxidation state on the catalytic activity of the $PdO_{x/2}/SiO_2$ samples for CO oxidation was examined. The rate of CO oxidation by O_2 to CO_2 was measured in the flowing mixture of CO and O_2 at 413 K. As shown in Fig. 7, the rates per gram of the $PdO_{x/2}/SiO_2$ samples decreased with the average oxidation number. Taking into account the result that the size of the Pd metal in the Pd/SiO_2 sample (21.1 nm) was larger than that of PdO in the PdO/SiO_2 sample (14.8 nm), the variation of activity was not originated from the variation of the Pd dispersion. The result in Fig. 7 indicates that the Pd^0 site is active species of the $PdO_{x/2}/SiO_2$ samples for CO oxidation under the present reaction conditions.

It should be noted that Pd L_3-edge XANES analysis is useful to quantify the average oxidation states of bulk and surface Pd species. The oxidation state of surface Pd species may change during the reaction at 413 K. To discuss the oxidation state of surface active Pd species, *in situ* IR with CO as a probe is the best characterization method.[12] Among various studies, a recent study by Zorn *et al.*[12b] is of

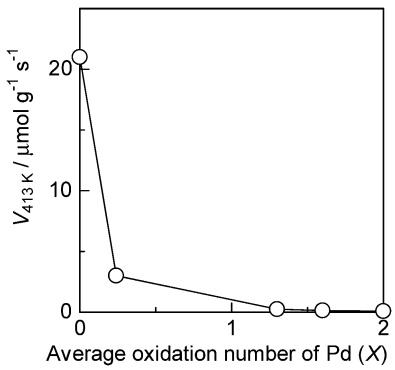

Fig. 7 Effect of the average oxidation number (x) of Pd in the $PdO_{x/2}/SiO_2$ catalyst on its reaction rate for CO oxidation at 413 K. Reaction conditions: 0.46% CO, 10% O_2.

importance, because it gives comprehensive results on the relationship between the Pd oxidation state and activity of PdO_y/Al_2O_3 (y = 0–1) catalysts for CO oxidation, whose conditions are similar to those in this study. They carried out *in situ* CO adsorption IR experiments at low temperature (100 K) after the pretreatment of PdO_y/Al_2O_3 catalysts under realistic CO oxidation conditions. Combining with various characterization results and density functional theory calculations, they concluded that the metallic Pd is responsible for the catalytic activity of Pd/Al_2O_3 for CO oxidation under realistic conditions at temperatures up to 553 K. Although our conclusion is not based on *in situ* characterization results, the results by Zorn *et al.*[12b] could support our conclusion that the Pd^0 site is active species of $PdO_{x/2}/SiO_2$ for CO oxidation under the reaction conditions.

The above discussion was based on the accurate oxidation number of the Pd species, which was determined by both the chemical method recorded during the catalyst preparation and the spectroscopic method recorded after the catalyst preparation. However, for the samples that are not applicable with the chemical method, such as Pd catalysts supported by highly reducible supports and Pd catalysts with transition metal additives, the spectroscopic method will be the only way to determine the accurate oxidation number. In this study, we presented a simple L_3-edge XANES analysis for the quantitative estimation of the average oxidation number of Pd species. It is claimed that, hereafter, this method will be available to discuss the effect of the Pd oxidation state on the activity of Pd catalysts, even when the determination of the Pd oxidation state is difficult by other characterization methods.

4. Conclusion

A simple method of Pd L_3-edge XANES analysis was examined to quantify the oxidation states of Pd species in a series of Pd-loaded SiO_2 catalysts containing different amounts of the Pd metal and PdO phases. The linear relationship between the average oxidation numbers determined by a chemical method (the number of CO_2 molecules formed during pre-reduction by CO) and the white line area intensities at L_3-edge Pd verifies that this method is effective for quantification of the average Pd oxidation number of unknown Pd species. This method reflecting the 4d-hole of Pd will become generally applicable to determination of the oxidation state of various Pd compounds.

Additionally, for the CO oxidation reaction by the $PdO_{x/2}/SiO_2$ (x = 0–2) samples, metallic Pd^0 sites are shown to be active species under the present reaction conditions.

Acknowledgements

The XAS measurements at Spring-8 were conducted with the approval of the Japan Synchrotron Radiation Research Institute (JASRI) (Proposal No. 2008B2066). The XAS measurements at KEK-PF were performed under the approval of the Photon Factory Program Advisory Committee (No. 2008G024). This work was supported by the Japanese Ministry of Education, Culture, Sports, Science and Technology *via* Grant-in-Aids for Scientific Research B (20360361) and for Young Scientists A (22686075).

References

1 E. Principi, A. Witkowska, S. Dsoke, R. Marassic and A. D. Cicco, *Phys. Chem. Chem. Phys*., 2009, **11**, 9987–9995.
2 H. Yoshitake and Y. Iwasawa, *J. Phys. Chem*., 1992, **96**, 1329–1334.
3 S. R. Bare, S. D. Kelly, B. Ravel, N. Greenlay, L. King and G. E. Mickelson, *Phys. Chem. Chem. Phys*., 2010, **12**, 7702–7711.
4 H. Yoshida, S. Nonoyama, Y. Yazawa and T. Hattori, *Phys. Scr*., 2005, **T115**, 813–815.
5 Y. Yazawa, N. Takagi, H. Yoshida, S. Komai, A. Satsuma and T. Hattori, *Appl. Catal., A*, 2002, **233**, 103–112.
6 T. Tanabe, Y. Nagai, K. Dohmae, H. Sobukawa and H. Shinjoh, *J. Catal*., 2008, **257**, 117–124.
7 J. Singh, E. M. C. Alayon, M. Tromp, O. V. Sofanova, P. Glatzel, M. Nachtegaal, R. Frahm and J. A. van Bokhoven, *Angew. Chem., Int. Ed*., 2008, **47**, 9260–9263.
8 E. Becker, P.-A. Carlsson, H. Grönbeck and M. Skoglundh, *J. Catal*., 2007, **252**, 11–17.
9 J.-D. Grunwaldt, M. Beier, B. Kimmerle, A. Baiker, M. Nachtegaal, B. Griesebock, D. Lützenkirchen-Hecht, J. Stötzel and R. Frahm, *Phys. Chem. Chem. Phys*., 2009, **11**, 8779–8789.
10 J. A. Anderson, B. Bachiller-Baeza and M. Fernández-García, *Phys. Chem. Chem. Phys*., 2003, **5**, 4418–4427.
11 (*a*) Y. Yazawa, H. Yoshida, S. Komai, A. Satsuma and T. Hattori, *Appl. Catal., B*, 1998, **19**, 261–266; (*b*) Y. Yazawa, H. Yoshida, N. Takagi, S. Komai, A. Satsuma and T. Hattori, *J. Catal*., 1999, **187**, 15–23.
12 (*a*) Y. Shen, G. Lu, Y. G. Yanqin, Y. Guo and X. Gong, *Catal. Today*, 2011, **175**, 558–567; (*b*) K. Zorn, S. Giorgio, E. Halwax, C. R. Henry, H. Grönbeck and G. Rupprechter, *J. Phys. Chem. C*, 2011, **115**, 1103–1111.
13 S. Hinokuma, H. Fujii, M. Okamoto, K. Ikeue and M. Machida, *Chem. Mater*., 2010, **22**, 6183–6190.
14 A. Iglesias-Juez, A. Kubacka, M. Fernández-García, M. D. Michiel and M. A. Newton, *J. Am. Chem. Soc*., 2011, **133**, 4484–4489.
15 S.-H. Oh and G. B. Hoflund, *J. Phys. Chem. A*, 2006, **110**, 7609–7613.
16 A. Iglesias-Juez, A. Martínez-Arias, M. A. Newton, S. G. Fiddy and M. Fernández-García, *Chem. Commun*., 2005, 4092–4094.
17 J.-D. Grunwaldt, L. Basini and B. S. Clausen, *J. Catal*., 2001, **200**, 321–329.
18 K. Dohmae, Y. Nagai, T. Tanabe, A. Suzuki, Y. Inada and M. Nomura, *SIA Surf. Interface Anal*., 2008, **40**, 1751–1754.
19 S. R. Bare and T. Ressler, *Adv. Catal*., 2009, **52**, 339–465.
20 M. Fernández-García, F. K. Chong, J. A. Anderson, C. H. Rochester and G. L. Haller, *J. Catal*., 1999, **182**, 199–207.
21 S. R. Bare, S. D. Kelly, F. D. Vila, E. Boldingh, E. Karapetrova, J. Kas, G. E. Mickelson, F. S. Modica, N. Yang and J. J. Rehr, *J. Phys. Chem. C*, 2011, **115**, 5740–5755.
22 E. Bus, R. Prins and J. A. van Bokhoven, *Phys. Chem. Chem. Phys*., 2004, **6**, 3903–3906.
23 I. Davoli, S. Stizza, A. Bianconi, M. Benfatto, C. Furlani and V. Sessa, *Solid State Commun*., 1983, **48**, 475–478.
24 T. Kubota, Y. Kitajima, K. Asakura and Y. Iwasawa, *Bull. Chem. Soc. Jpn*., 1999, **72**, 673–681.
25 M. W. Tew, J. T. Miller and J. A. van Bokhoven, *J. Phys. Chem. C*, 2009, **113**, 15140–15147.
26 K. Okumura, T. Tomiyama, S. Okuda, H. Yoshida and M. Niwa, *J. Catal*., 2010, **273**, 156–166.
27 L. C. Witjens, J. H. Bitter, A. J. van Dillen, K. P. de Jong and F. M. F. de Groot, *Phys. Chem. Chem. Phys*., 2007, **9**, 3312–3320.
28 T. Miyamoto, H. Niimi, Y. Kitajima, T. Naito and K. Asakura, *J. Phys. Chem. A*, 2010, **114**, 4093–4098.
29 K. Shimizu, T. Oda, Y. Sakamoto, Y. Kamiya, H. Yoshida and A. Satsuma, *Appl. Catal. B*, 2012, **111–112**, 509–514.
30 K. Shimizu, H. Maeshima, H. Yoshida, A. Satsuma and T. Hattori, *Phys. Chem. Chem. Phys*., 2000, **2**, 2435–2439.
31 D. Bazin and L. Guczi, *Appl. Catal., A*, 2001, **213**, 147–162.
32 J. Chen, E. Kemly, M. Croft, Y. Jcon, X. Xu, S. A. Shaheen and P. H. Ansari, *Solid State Commun*., 1993, **85**, 291–296.
33 T. Tanabe, Y. Nagai, T. Hirabayashi, N. Takagi, K. Dohmae, N. Takahashi, S. Matsumoto, H. Shinjoh, J. N. Kondo, J. C. Schouten and H. H. Brongersma, *Appl. Catal., A*, 2009, **370**, 108–113.
34 B. K. Teo, *EXAFS: Basic Principles and Data Analysis*, Springer-Verlag, Berlin, 1986.

